Channel Estimation Method with Improved Performance for the UMTS-TDD mode

P. Marques[1,2], A. Gameiro[2] and J. Fernandes[2]

Abstract - Channel estimation is an essential building block for UTRA-TDD high performance receivers. Once the performance of the channel estimator algorithm proposed by 3GPP is highly dependent on the time spreading between consecutive multi-path components, a Successive Multi-path channel Estimation Technique (SMET) that improves the time resolution is proposed in this paper. A SMET based maximum likelihood approach for vectorial channel estimation, to include the estimation of the direction-of-arrival, is also proposed. This algorithm solves efficiently the complex problem of *DOA* estimation of multiple users in a multi path propagation environment even when the number of required *DOA's* exceeds the number of antenna array elements. Another property of the proposed algorithm is its ability to resolve signals from different users arriving from the same direction. This is due to processing in both time and space dimensions. The performance of these algorithms is assessed by resorting to simulations in multi-path environments using the UMTS-TDD specifications, and also by comparing the *rms* estimation errors against the Crámer-Rao Bound. The effect of imperfect channel estimation on the performance of RAKE and Hard-Decision Parallel Interference Canceller receivers is also analysed. The results show that a good performance can be achieved with SMET, from low to high values of Eb/n_0.

Key words — Channel estimation, direction-of-arrival, maximum-likelihood methods, multi-path channels, UMTS-TDD.

I. INTRODUCTION

The UMTS Terrestrial Radio Access (UTRA) consists of two modes, a frequency division duplex (FDD) and a time division duplex (TDD). The FDD mode is intended for applications in public macro and micro cell environments with data rates of up to 384 Kb/s and high mobility. The TDD mode is advantageous for public micro and pico cell environments and for wireless local loop applications. It facilitates an efficient use of the

[1] Escola Superior de Tecnologia – Instituto Politécnico de Castelo Branco, 6000 Castelo Branco, Portugal

[2] Universidade de Aveiro, Instituto de Telecomunicações / DETUA, 3810 Aveiro, Portugal

unpaired spectrum and supports data rates up to 2 Mb/s. Therefore the TDD mode is particularly well suited for environments with high traffic density and indoor coverage, where the applications require high data rates and tend to create highly asymmetric traffic patterns [1].

In mobile radio the transmitted signal is scattered by many obstacles thus creating a multi-path channel. Accurate multi-path channel estimation is therefore a key issue for the advanced signal processing techniques proposed for UMTS to achieve a good performance, e.g., RAKE and Multiuser Detection (MUD) receivers [2], array processing [3], power control and high-accuracy wireless position location services proposed by 3GPP [4].

Several techniques can be employed to increase the link capacity of UMTS-TDD systems, namely through the use of antenna arrays [3] or MUD receivers. However, to exploit efficiently the energy in the different propagation paths it is necessary to estimate the relative delays, and subsequently, the phase and amplitude of each multi-path component. In the case of array receivers, there is an additional requirement to provide accurate estimates for the direction-of-arrival of the multi-path components impinging on the antenna array. All these advanced signal processing techniques, including the conventional RAKE receiver, require an accurate multi-path channel estimator to achieve a good performance.

The channel estimation algorithm proposed in this paper is based on the standard one suggested by 3GPP for UTRA-TDD. For this mode, the burst structure specifies a specially designed midamble to allow channel estimation by cyclic correlation [5]. As it will be shown in section III the performance of this algorithm is highly related with the temporal spreading between consecutive paths. A Successive Multi-path channel Estimation Technique (SMET) is proposed to replace the 3GPP scalar channel estimator. In addition, a method to define a threshold level in order to activate only the RAKE fingers with sufficiently high Signal to Interference plus Noise Ratio (*SINR*) is proposed as well as a simple *SINR* estimator based on channel estimates. A Maximal Likelihood (ML) extension to SMET is also proposed to perform the direction-of-arrival (*DOA*) estimation. ML techniques are optimal techniques and perform well even under low *SINR* conditions, typical of CDMA systems, but are computationally very demanding [6]. To overcome this limitation a moderate complexity ML direction-of-arrival estimation based on SMET is implemented. These algorithms were implemented and integrated in a link level evaluation platform for the UTRA-TDD physical layer following current 3GPP specifications [7].

The paper is organized as follows. In section II we present the system model. Section III describes the conventional 3GPP Complex Impulse Response (CIR) estimation algorithm. Then in Section IV the SMET proposal is presented and described for the scalar channel case, while the extension to vectorial channels is considered in section V using the ML principle to estimate the direction-of-arrival. In section VI, resorting to

simulations, we present numerical results to illustrate the algorithm's performance. The measured results are compared against the Crámer-Rao Bound (*CRB*) which is derived. Furthermore the impact of the estimator errors on the bit error rate (BER) performance of the RAKE, and Hard-Decision Parallel Interference Canceller (HD-PIC) is also addressed. Finally the main conclusions are outlined in Section VII.

II. SYSTEM MODEL

Figure 1 shows the block diagram of the uplink system model we shall be dealing with. We consider *K* single antenna mobiles communicating with the base station which uses an antenna array of *M* sensors arranged in a circular geometry The channel estimation unit provides outputs to the space-time equalization / detection units about the *K* uplink channels.

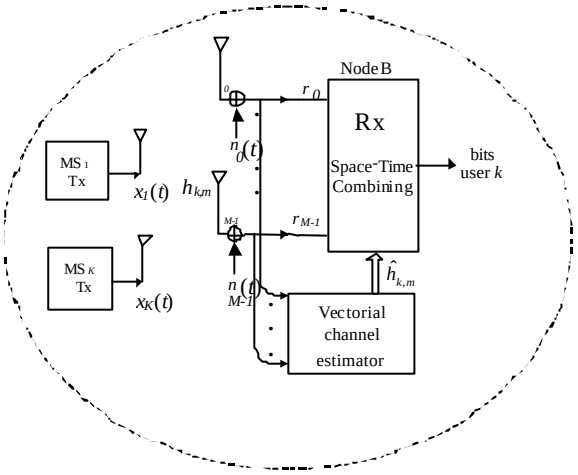

Fig.1. Cell system model structure.

In the UTRA-TDD mode, the burst structure includes two data fields and a specially designed midamble to allow channel estimation by cyclic correlation. The 3GPP specification documents defines two types of bursts, Type 1 and Type 2. The length of the midamble *Lm* distinguishes them, 512 chips for Burst-Type 1 and 256 chips for Burst-Type 2 [5]. The complex base-band representation of the *k*th user's transmitted TDD burst is given by,

$$x_k(t) = \sqrt{P_k}\left\{\sum_{i=1}^{Ns} d_{k,i}\, c_k(t - i\,SF\,T_c) + \sum_{i=Ns+1}^{Ns+Lm} M_k(i - Ns - 1)\, g(t - i\,T_c) + \sum_{i=Ns+Lm+1}^{2464} d_{k,i}\, c_k(t - i\,SF\,T_c)\right\} \quad (1)$$

where P_k is the transmitted power, T_c the chip duration 260 ns, $d_{k,i} \in \{1,j,-1,-j\}$ the ith data transmitted QPSK symbol and $M_k = \{M_k(0) \quad \ldots \quad M_k(Lm-1)\}$ is the complex midamble code. Ns denotes the number of QPSK symbols transmitted per data field,

$$Ns = \begin{cases} \frac{976}{SF}, & \text{Burst-Type 1} \\ \frac{1104}{SF}, & \text{Burst-Type 2} \end{cases} \qquad (2)$$

where SF represents spreading factor.

For the data field the spreaded waveforms $c_k(t)$ of SF chips are given by

$$c_k(t) = \sum_{n=0}^{SF-1} S_n C_{k,n} g(t - nT_c) \qquad (3)$$

where $C_{k,n} \in \{1,-1\}$ is the nth element of the kth channelisation code, S_n is the nth element of the scrambling code and $g(t)$ is the impulse response of the root raised cosine shaping filter with a roll-off factor of 0.22. The scrambling code S_n is the same for all users in a cell.

The received signal at the Node B is a superposition of multiple copies of attenuated and delayed signals transmitted by all K users. The radio channel of each user in multi-path environment can be modelled by a tap-delay-line [8],

$$h_{k,m}(t) = \sum_{l=1}^{L} a_{k,l} \, e^{\,j\Omega_{k,l,m}} d(t - t_{k,l}) \qquad (4)$$

where:

m:(0...M-1) refers to the mth array element

k:(1..K) refers to the kth user

l:(1...L) refers to the lth channel path

$a_{k,l}$ is the amplitude of the lth multi-path component of user k which is considered identical for the all M elements, i.e., $a_{k,l} \approx a_{k,l,m}$

$\Omega_{k,l,m} = q_{k,l} + a_m(f_{k,l})$ where $q_{k,l}$ is the phase of the l*th* multi-path component of user k and $a_m(f_{k,l})$ is the phase shift relatively to m=0 array sensor for the direction-of-arrival $f_{k,l}$ measured in azimutal plane.

$t_{k,l}$ is the path lth delay of user k which is considered identical for the all M elements, i.e., $t_{k,l} \approx t_{k,l,m}$

Therefore, the signal at the mth array sensor is given by,

$$r_m(t) = \sum_{k=1}^{K} \sum_{l=1}^{L} a_{k,l} e^{j\Omega_{k,l,m}} x_k(t - t_{k,l}) + n_m(t) \qquad (5)$$

The additive noise processes present at each antenna $n_m(t)$, are assumed to be uncorrelated white noise complex Gaussian with zero mean and power spectral density n_0. In this system model $n_m(t)$ also includes the intercell interference due to other cells. The M signals received at each Node B antenna are processed by a space-time combing technique [6]. The block diagram shown in Figure 1 comprises the vectorial channel estimation unit that will be analysed hereafter.

III. CONVENTIONAL UTRA-TDD CIR ESTIMATION ALGORITHM

The block diagram for the CIR estimation unit proposed by 3GPP [5] is shown in Figure 2.

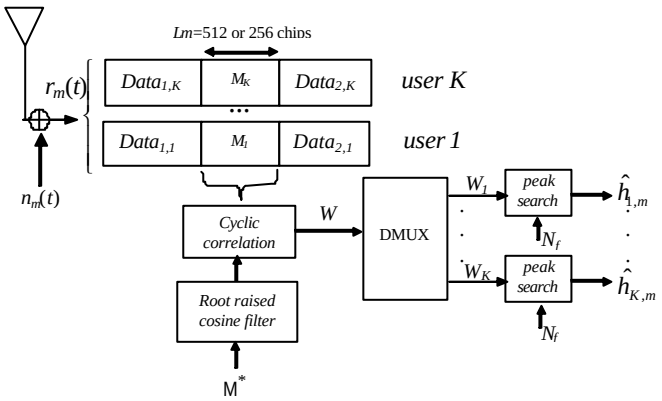

Fig.2 GPP Complex Impulse Response estimation unit.

The midambles of different users active in the same time slot (M_k) are time-shifted versions of one single periodic basic code, M. The 3GPP specification document defines a length for M of 456 chips for Burst-Type 1 and 192 chips for Burst-Type 2 [5] [9]. Different cells use different uncorrelated periodic basic codes. This allows the joint estimation for the channel impulse responses of all active users within one time slot which can be done by a single cyclic correlation (Figure 2). The output of the correlation operation between the received midamble field and the local version of the (shaped) basic code is a vector $W=[W_1,\ldots,W_K]$ where each element W_k is a vector corresponding to a time window with length and time duration defined in Table I. The different user specific channel impulse response estimates are obtained in a specific W_k chip window as shown in Figure 2 (DMUX operation). If the receiver is based on a RAKE employing N_f fingers ($N_f \leq L$), then the most straightforward approach would be to search for the N_f dominant peaks in each W_k chip window. The locations and complex amplitudes of these peaks constitute the delay estimates, $t_{k,l}$, amplitude $a_{k,l}$, and phase $\Omega_{k,l}$ of the *lth* multi-path component of the user k.

The higher layers perform the specification of the midambles to be used within a cell. The main characteristics of the midambles are summarized in Table I.

TABLE I

SUMMARY OF THE MIDAMBLE CHARACTERISTICS

Burst-Type 1 Lm=512 T_c	K=8; W_k chip window=57T_c Max delay 15 us	
Burst-Type 2 Lm=256 T_c	K=3; W_k chip window=64T_c Max delay 16.6 us	K=8; W_k chip window=24T_c Max delay 6.2 us

Burst-Type 1 is suited for uplink transmission while Burst-Type 2 was designed to be used typically in the downlink, however 3GPP specifications indicate that is possible to use Burst-Type 2 for uplink, but only if the burst is allocated to less than four users [5]. In this paper we propose that Burst-Type 2 can be used also in uplink transmission, even with K=8 (see third column in Table 1). If we consider more intermediate shifts in the midamble basic code, then Burst-Type 2 is long enough to provide 8 channel estimations with maximum delay less that 24T_c, which is sufficient for Indoor and Pedestrian A, B and Vehicular A channels proposed by ETSI [10]. It should be noted that Burst-Type 2 transmission effectively increases the length of data fields relatively to Burst-Type 1 (see (2)) which results in a higher throughput. The drawback to extend Burst-Type 2 (shorter

midamble) to uplink is the decrease of maximum delay spread supported by channel estimator and possible degradation of the estimates when compared to Burst-Type 1 (longer midamble). However, Section VI will show that the effect of burst type on BER performance is practically negligible if the delay spread of the CIR is low enough.

To assess the resolution capability of the algorithm, we considered a "two-wave" (L=2) scenario. Considering a noise free situation, the W_k chip window at the 3GPP output correlator can be written as (in this section to simplify the notation we will omit index m referring the antenna element):

$$W_k(t) = \sum_{l=1}^{2} a_{k,l} e^{j\Omega_{k,l}} \sum_{i=0}^{Lm-1} \Gamma_k(i)\, G(t - iT_c - t_{k,l}) \qquad (6)$$

where G is the impulse response of the raised cosine shaping filter and Γ_k is the autocorrelation function of M_k midamble code given by,

$$\Gamma_k(i) = \sum_{j=0}^{Lm-1} M_k(j) M_k^*(j+i) \approx \begin{cases} Lm, & i = 0 \\ 0, & i \neq 0 \end{cases} \qquad (7)$$

Furthermore to obtain (6) we have considered that the K different midamble codes are orthogonal.

The correct/incorrect estimation analysis is made in the worst case, that is, when two waves arrive in phase and their resolution is more difficult. In this analysis it is considered the following maximum error criterion: 15% for amplitude estimation and $T_c/4$ for delay estimation, i.e., a correct estimation occurs when the two paths verify: $\left|a_{k,l} - \hat{a}_{k,l}\right| < 0.15 a_{k,l} \wedge |t_{k,l} - \hat{t}_{k,l}| < T_c/4$; where $\hat{a}_{k,l}, \hat{t}_{k,l}$ denote the estimates obtained. Figure 3 shows the 3GPP channel estimation error plane. The number of samples per chip (N_c) is 4.

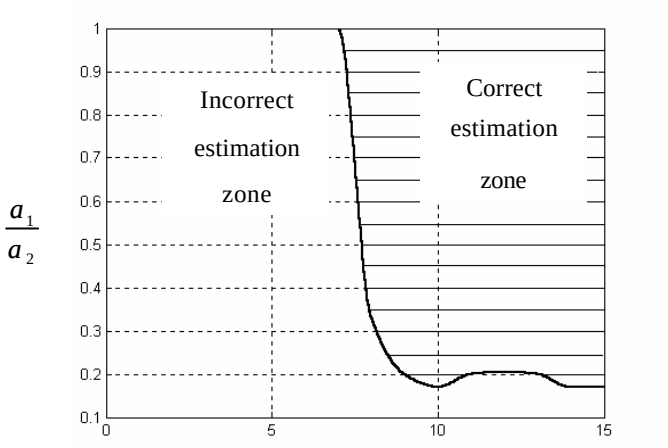

Fig.3. Conventional 3GPP channel estimation error plane (noise free).

Due to the shaping filter bandwidth limitation (B), the 3GPP scalar estimation algorithm can only resolve multi-path components if they are separated by more than $\Delta t \approx 1/B = 2\ T_c$ which is 520 ns for UMTS. On the other hand, in the peak search process, the secondary lobules of the raised cosine chip filter can be interpreted as false paths components if the amplitude ratio between two paths is less than 0.2 (-14 dB). This case can be seen in Figure 4.

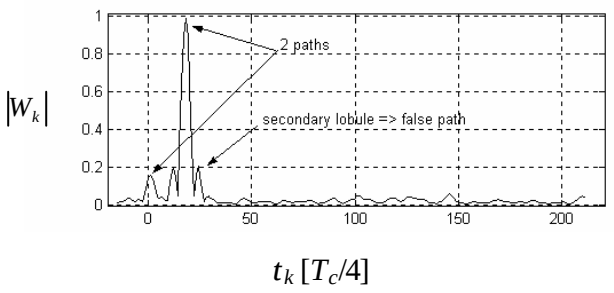

Fig.4. Typical $|W_k|$ chip window: secondary lobule is interpreted as false signal path.

IV. SUCCESSIVE MULTI-PATH ESTIMATION TECHNIQUE

Measurements have shown that in Indoor and Pedestrian environments the temporal spacing between consecutive paths may be less than 520 ns [10]. To accommodate such scenarios we propose to modify the 3GPP algorithm in order to improve the time resolution. We name this technique as SMET and it

works as follows: successively search the highest peak of the W_k chip window produced by the output correlator and subtract to the overall waveform the elementary pulse with the parameters obtained from the highest peak. This operation may be repeated N times. With such a scheme the accuracy of the multi-path estimates improve at the output of the successive multi-path cancellation stages. This technique has evident similarities with the soft decision successive interference cancellation (SIC) [11] used in multi-user detection. The SMET algorithm for two fingers consists in applying the following procedure (the extrapolation for N_f fingers is straightforward):

$$
\begin{aligned}
&W_1(t) = W_k(t)\\
&\textit{for } i = 1 \textit{ to } \mathrm{N}\\
&\quad \hat{a}_{k,1}^{(i)} = \max \left|W_1(t)\right|\\
&\quad (\hat{\Omega}_{k,1}^{(i)}, \hat{t}_{k,1}^{(i)}) = \arg\max \left|W_1(t)\right|\\
&\quad W_2(t) = W_1(t) - \hat{a}_{k,1}^{(i)} e^{j\hat{\Omega}_{k,1}^{(i)}} G(t - \hat{t}_{k,1}^{(i)})\\
&\quad \hat{a}_{k,2}^{(i)} = \max \left|W_2(t)\right|\\
&\quad (\hat{\Omega}_{k,2}^{(i)}, \hat{t}_{k,2}^{(i)}) = \arg\max \left|W_2(t)\right|\\
&\quad W_1(t) = W_k(t) - \hat{a}_{k,2}^{(i)} e^{j\hat{\Omega}_{k,2}^{(i)}} G(t - \hat{t}_{k,2}^{(i)})\\
&\textit{end}
\end{aligned}
$$

A. Time resolution

Figure 5 depicts the SMET error plane, with two stages (N=2), and it shows that a significant improvement is achieved with the proposed technique. Moreover, it is also quite robust to the secondary lobules effect, as seen by the extension of the correct zone in the amplitude domain. This multi-path discrimination technique has a low algorithmic complexity, and does not impact significantly the overall complexity of the scalar channel estimator.

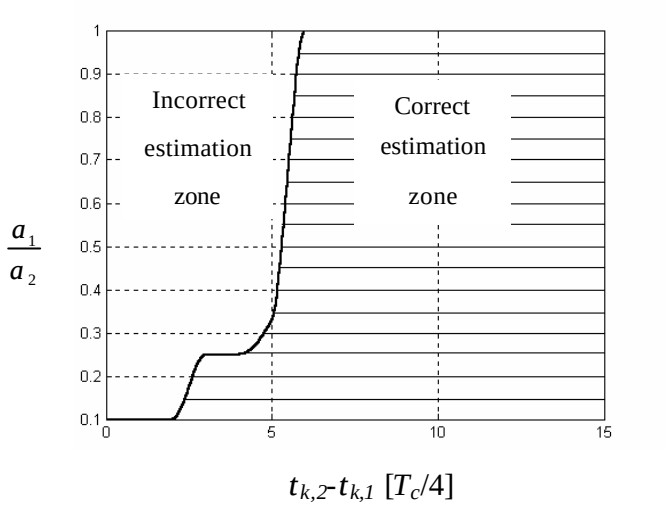

Fig.5. SMET error plane N=2 (noise free).

B. Crámer-Rao Bound for amplitude and delay estimatives

The *CRB* was derived and computed to provide a theoretical benchmark to assess the performance of the algorithm relatively to the optimum case. The *CRB* provides a lower bound on the *rms* error for any unbiased estimator, thus providing a value indicating the best performance that can be achieved by any unbiased estimator. The *CRB*s are derived in the Appendix A. In Figures 6-7, the rms error of the amplitude and delay estimates is given, together with the *CRB* of these parameters. A Signal to Noise Ratio at W_k chip window (SNR_0) equal to 20 dB and two-path channel with $a_{k,1}e^{j\Omega k,1}=a_{k,2}e^{j\Omega k,2}$ (worst case) is considered. The *rms* error for the amplitude and delay is given by,

$$s_{a_k error} = \sqrt{\frac{1}{L\,Y}\sum_{l=1}^{L}\sum_{i=1}^{Y}\left(\frac{a_{k,l,i}-\hat{a}_{k,l,i}}{a_{k,l,i}}\right)^2} \qquad (8)$$

$$s_{t_k error} = \sqrt{\frac{1}{L\,Y}\sum_{l=1}^{L}\sum_{i=1}^{Y}\left(t_{k,l,i}-\hat{t}_{k,l,i}\right)^2} \qquad (9)$$

where Y is the number of UMTS-TDD bursts simulated.

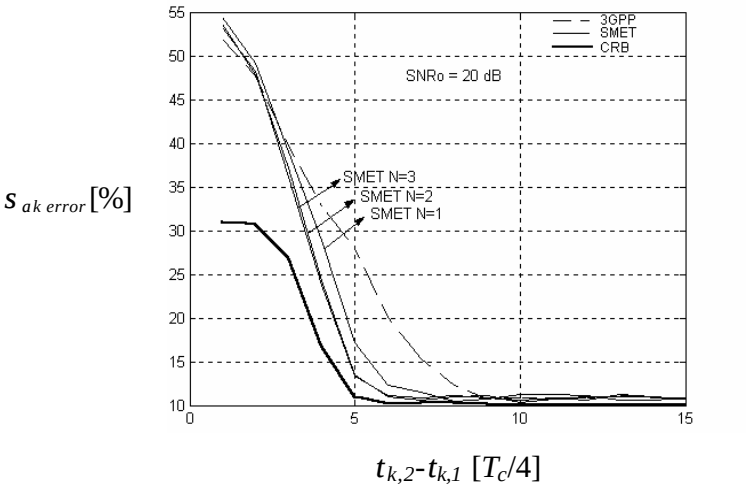

Fig.6. rms error amplitude for SMET and 3GPP estimators against Crámer-Rao bound, $a_{k,1}e^{j\Omega_{k,1}}=a_{k,2}e^{j\Omega_{k,2}}$.

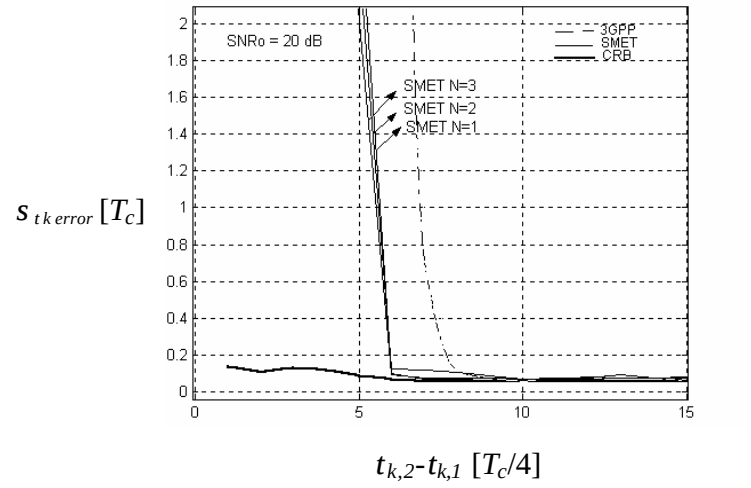

Fig.7. rms error delay for SMET and 3GPP estimators against Crámer-Rao bound, $a_{k,1}e^{j\Omega_{k,1}}=a_{k,2}e^{j\Omega_{k,2}}$.

Considering the maximum error criterion: 15% for amplitude and T_c/4 for delay, the time resolution for 3GPP conventional algorithm is $2T_c$, while $3T_c$/2 is achieved with SMET (N=2). However it should be noted that the *CRB* for time resolution is equal to $1T_c$. For SMET, simulations have shown that increasing the number of stages (N > 2) provided a negligible performance improvement.

C. Threshold level formulation

Figure 8 shows a typical sequence of SMET computation. Figure 8-(a), clearly shows the existence of peaks that are caused by noise and interference, which could be interpreted as false paths contributing with additional interference in the receiver and consequently degrading the BER [12]. To minimize this problem a threshold level (TH) is included in order to activate only the fingers with sufficiently high signal-to-interference plus noise per path: defined as $g_{k,l}=a_{k,l}^2/s_n^2$.

After the SMET the residual chip window is given by:

$$W_{0k}(t)=W_k(t)-\sum_{l=1}^{N_f}\hat{a}_{k,l}e^{j\hat{\Omega}_{k,1}}G(t-\hat{t}_{k,l}) \qquad (10)$$

$W_{0k}(t)$ accounts for several disturbances: the additive white Gaussian noise present at the antenna input, the intracell interference due to other users within one time slot, the intercell interference due to other cells with different M codes, and the channel estimation errors. Let us consider in the analysis that $W_{0k}(t)$ is Gaussian distributed with variance s_n^2, then

$$P(|W_{0k}|\le \mathrm{TH})=1-e^{-\frac{\mathrm{TH}^2}{2s_n^2}} \qquad (11)$$

Defining a parameter p as the tolerable probability for a false path, immediately defines the threshold level as:

$$\mathrm{TH}=\sqrt{-2s_n^2\ln(p)},\quad 0<p\le 1 \qquad (12)$$

The parameter p needs to be chosen in order to maximize system performance, in [18] it is used $p=10^{-4}$. Figure 8 shows the sequence of threshold level computation. In this example the second path has a low $g_{k,l}$, thus it ends up to be eliminated by the threshold processing. Notice that the number of multi-path components is not assumed known a priori. $\hat{L}$ is given by threshold operation, in this case $\hat{L}=1$, but $N_f=2$.

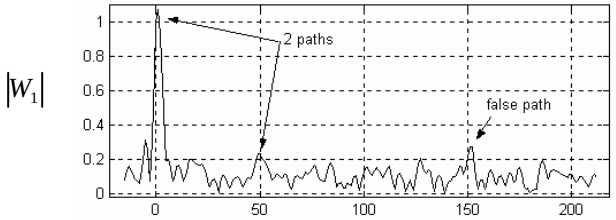

(a)

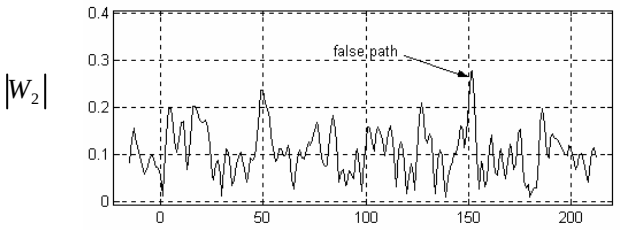

(b)

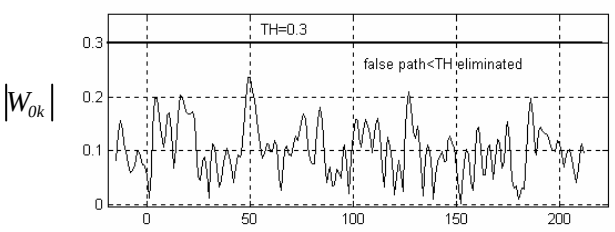

(c)

Fig.8 (a) $|W_1|$ chip window; conventional 3GPP channel estimator, (b) $|W_2|$: chip window after strong path elimination (c)$|W_{0k}|$: residual chip window; threshold level calculated with p=10^{-4} [18].

V. VECTORIAL CHANNEL ESTIMATOR

The CIR estimator algorithm previously described was extended to estimate also the *DOA* of the multi-path components.

A. Blind estimation algorithms

Various algorithms to estimate the *DOA* can be found in literature. The most popular uses blind subspace-based techniques to exploit the eigen structure of the input covariance matrix, for example MUSIC and ESPRIT. The most significant drawbacks of the subspace-based techniques are [6] [19]:

- These methods degrade severely in a multi-path propagation environment, especially with low *SINR*.
- *M* element array can only detect *M*-1 non-correlated signals.
- Require that the number of signals impinging on the array be known or estimated.

- Limited angular resolution: for both algorithms the *DOA* estimation error increase as the angular separation of the signals decreases.

The most common DOA estimation methods (see [19] and references therein) are based on the assumption that the number of antennas is greater than the number of spatially separated interfering signals. Unfortunately, this assumption is not valid in most, if not all, multiple-acess systems where the number of active users can certainly exceed the number of antennas and the radio channels have several independent paths.

B. Midamble aided maximum likelihood parameters estimation

Since ML techniques are computationally intensive they are less popular than suboptimal subspace techniques. However, recently, a number of channel estimation algorithms based on ML criterion have emerged [20] [21]. The straightforward application of ML parametric estimation of L multi-path components (with parameters $f_{k,l}$, $a_{k,l}$ and $t_{k,l}$) that arrive at the receiver from K users results in a KxLx3-dimensional maximisation problem, which is computationally prohibitive. To simplify the computation we propose to separate the temporal estimation, performed by SMET, to the spatial estimation (*DOA*), performed by ML criterion. The basic structure is shown in Figure 9; it simply consists in applying the SMET to each of the M array elements, and then estimate the $f_{k,l}$ using the maximum likelihood criterion based on the phase shift relation existing between array elements.

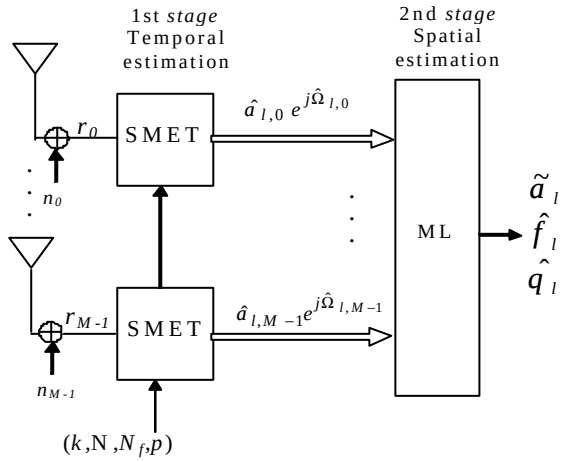

Fig.9. Vectorial channel estimation based in SMET.

This algorithm is of course no longer the optimum joint parameter estimator but it brings down the KxLx3-dimensional maximization problem to KxL successive 3-dimensional problems, thus reducing the computational complexity. In this algorithm, no *apriori* assumption is made on the geometry of the array. However, it is assumed that the envelope characteristics of the signal do not vary across the array elements.

The ML problem consists of joint estimation of the unknown parameters (in this section to simplify the notation we will omit index k referring the user), i.e: $u=[a_l, f_l, q_l]$; while the delay t_l is estimated by SMET (1st stage; Temporal estimation). Let $\vec{h}_l=[\Psi_{l,0} \ldots \Psi_{l,M-1}]$ be the 1xM observation vector, relatively to l path channel component, measured by the M SMET units of Figure 9. Each element of $\vec{h}_l$ is given by,

$$\Psi_{l,m} = \hat{a}_{l,m}\, e^{\,j\hat{\Omega}_{l,m}} = a_l\, e^{jq_l} e^{j a_m(f_l)} + \Delta_{l,m} \qquad (13)$$

where $\Delta_{l,m}$ is a complex estimation error. For simplicity analysis we assume $\Delta_{l,m}$ Gaussian with distribution $N(0,s_\Delta^2)$. $\hat{\Omega}_{l,m}$ is the total phase estimated for the lth path by the SMET unit in the mth array element. The M sources of error are assumed to be statistically independent. The application of ML criterion for f_l estimation seeks to find the maximum of the conditional probability function:

$$P(\vec{h}_l \mid u) = \prod_{m=0}^{M-1} \frac{1}{\sqrt{2p}\,s_\Delta} \exp\left[-\frac{1}{2s_\Delta^{\,2}} \left| \Psi_{l,m} - a_l\, e^{\,jq_l}\, e^{\,j a_m(f_l)} \right|^2 \right] \qquad (14)$$

which results as explained in Appendix B, in a Minimum Mean Square Error (MMSE) criterion,

$$(\tilde{a}_l, \hat{f}_l, \hat{q}_l) = \underset{a_l, f_l, q_l}{\arg\min} \sum_{m=0}^{M-1} \left| \Psi_{l,m} - a_l e^{jq_l} e^{j a_m(f_l)} \right|^2 \qquad (15)$$

and after some mathematical manipulations detailed in Appendix B we get

$$\tilde{a}_l = \frac{1}{M} \sum_{m=0}^{M-1} \hat{a}_{l,m} \qquad (16)$$

$$(\hat{f}_l, \hat{q}_l) = \underset{f_l, q_l}{\arg\max} \sum_{m=0}^{M-1} \hat{a}_{l,m} \cos\left(q_l + a_m(f_l) - \hat{\Omega}_{l,m}\right) \qquad (17)$$

It should be noted that maximisation of (17) is a 3D numerical search problem computationally viable. To obtain the angular resolution equal to Δf degrees the algorithm searches the maximum in $(360^o/\Delta f)^2$ points.

The performance of the ML-*DOA* estimation technique depends heavily on the quality of the estimates $\vec{h}_l$ provided by SMET. To improve the *DOA* estimation accuracy we included a threshold operation in order to active only ML criterion if estimated paths have sufficiently high g_l. Therefore, when one path component is eliminated by threshold process, we propose to use the f_l estimation obtained in the previous burst as the estimation for current burst. This technique allows reducing the *DOA* error but assumes some time coherence across some bursts. This is a reasonable assumption in low mobility scenarios which have been confirmed by numerous measurement campaigns [6] [14].

VI. Simulation Results

A. Channel model

The CIR estimation unit was implemented and integrated in a UMTS-TDD simulation platform. To assess its performance, simulations have been carried out, using a statistical 2D space-time channel. The parameters related to the radio channel are listed in Table II. To examine the effect of multi-path diversity the channel impulse response is normalized in power and includes two paths (L=2) with equal mean power and uncorrelated Rayleigh fading. The Doppler spectrum follows a classical Clarke model and the mobile velocity was set equal to 3 Km/h. The time separation between paths is t_2-t_1=5T_c/4. The power azimuth spread of the signal seen from the Node B is Laplacian distributed as proposed by COST 259 [13]. Based on [14] proposal for microcelular pedestrian environments we assume angular spread (A) equal to 15º and the mean azimuth f_l equal to 2º and -20º for path 1 and path 2 respectively.

TABLE II Summary of the channel parameters

$E[a_1^2]=E[a_2^2]$	t_2-t_1	$E[f_1]$	$E[f_2]$	A
-3 dB	5T_c/4	2º	-20º	15º

B. Effect of channel estimation on BER

A link level simulation chain was used to analyse the effect of imperfect channel estimation on the overall link BER versus Eb/n_0 as shown in Figure 10 and Figure 11. The simulation scenario includes K=1 and K=8 users with equal mean power and identical spreading factor (16) and both Burst-Type 1 and Burst-Type 2 were considered. Two receiver structures were analyzed: RAKE receiver with N_f=2 whose results are shown in Figure

10 and multi user detector HD-PIC with one cancellation stage [16], with the respective results shown in Figure 11. In both plots include the BER obtained using the channel estimates provided by the estimator and the BER obtained assuming perfect knowledge of the channel characteristics to quantify the degradation introduced by the estimation process.

Due to time resolution improvement, the BER performance with SMET clearly outperforms the 3GPP channel estimator. It can be seen from Figure 10 and Figure 11 that in a perfectly known channel the HD-PIC receiver outperform the RAKE receiver; however we can see that HD-PIC is more sensible to the channel estimation errors as shown in [17]. The improvement achieved using Burst-Type 1 (long midamble) instead of Burst-Type 2 (short midamble) is nearly negligible: 0.5 dB for RAKE receiver with K=1 and 0.8 dB for HD-PIC with K=8 for BER=10^{-2}.

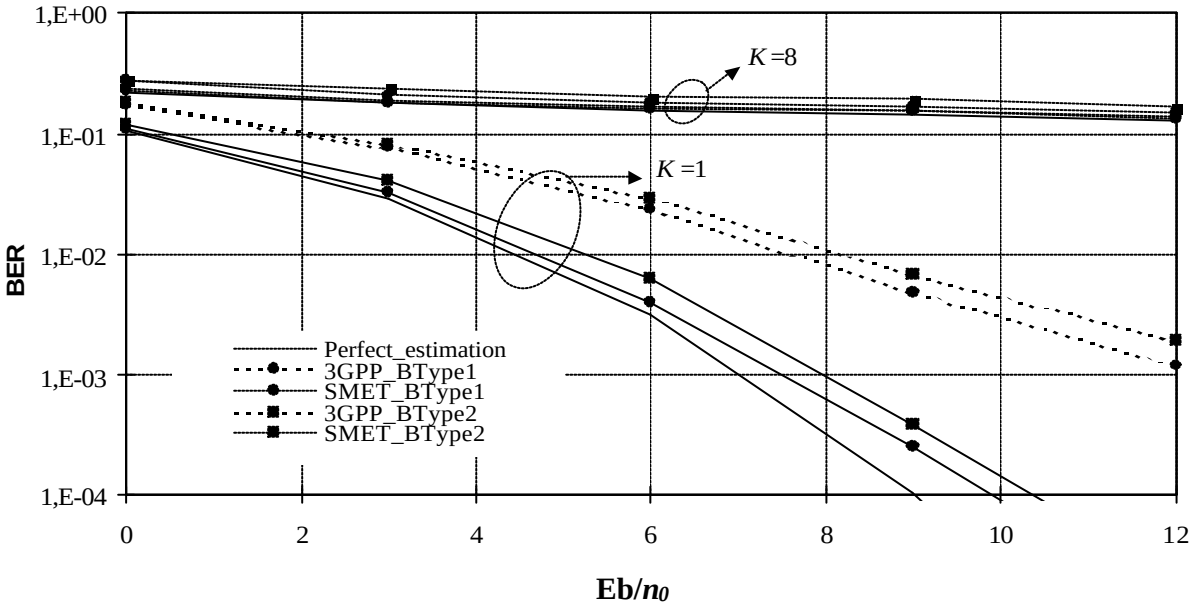

Fig.10 RAKE with 2 fingers, K=1,8 users, SF=16.

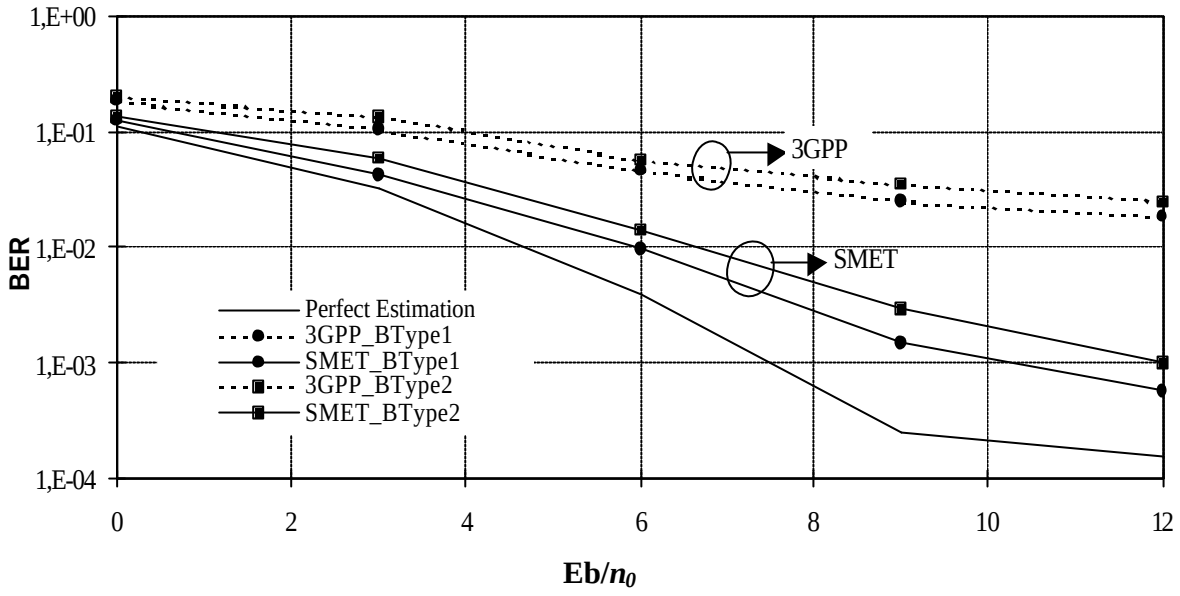

Fig. 11 Hard-Decision PIC, K=8 users with equal power, SF=16.

C. *DOA* estimator performance

For the particular case of a Uniform Circular Array (UCA) with an inter-element space d and M equally spaced elements, the steering vector in the horizontal plane is given by [6],

$$a_m(f_l) = -\frac{2p}{l} d \cos(f_l - 2p \frac{m}{M}) \qquad (18)$$

For the simulations we considered a UCA with M=8 antennas with an inter-element space of $d = l/2$. The simulations and the *CRB* computation (see Appendix C) were performed for two-path Rayleigh channels with t_2-$t_1 \in \{1T_c, 5T_c/4, 2T_c\}$, and both cases, with and without threshold operation were tested. For the threshold operation we considered for the probability of false path indication, p=10^{-4}. The *rms* error for the *DOA*,

$$s_{f\,error} = \sqrt{\frac{1}{K\,L\,Y}\sum_{k=1}^{K}\sum_{l=1}^{L}\sum_{i=1}^{Y}\left(f_{k,l,i} - \hat{f}_{k,l,i}\right)^2} \qquad (19)$$

where *Y* is the number of UMTS-TDD bursts simulated is plotted as a function Eb/n_0 in Figure 13. The *CRB* and *rms* error parameters are averaged over 1000 UMTS-TDD burst. The ML search problem was used with 1º resolution. It is evident from Figure 13 that as the Eb/n_0 level increases the *rms* error estimation error decreases and also shows that the estimates are relatively close to the Cramér-Rao Bound. The performance of ML estimator can be significantly improved if threshold operation is included in SMET.

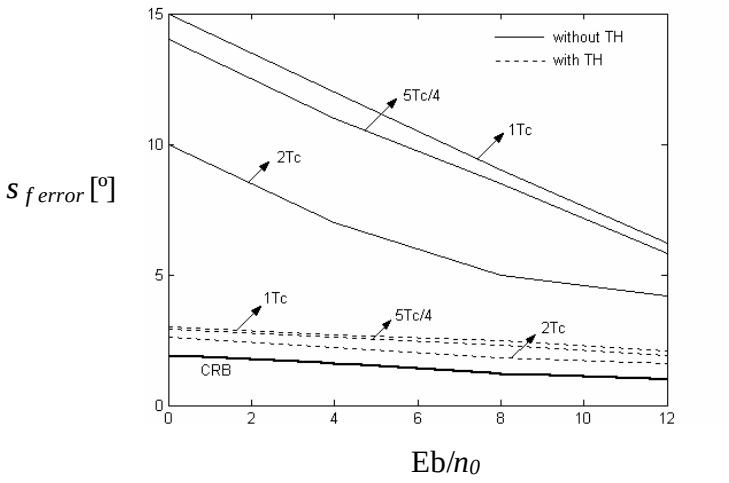

Fig.13. *DOA* rms error for ML Estimation based on SMET and *CRB*; *K*=1 user, Burst-Type 1.

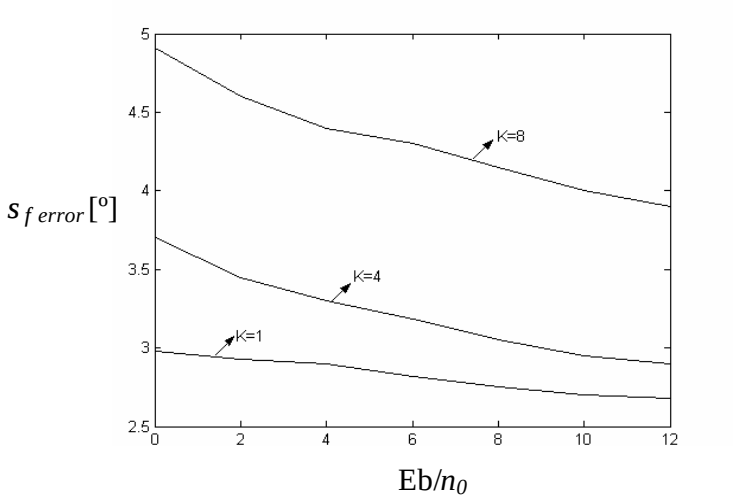

Fig.14. *DOA* rms error for ML Estimation with threshold operation for *K*=1, 4 and 8 users, Burst-Type 1.

VII CONCLUSIONS

In this paper we considered a new channel estimator for UMTS-TDD that overcomes some of the limitations of the conventional 3GPP channel estimator. The conventional 3GPP channel estimation algorithm is highly limited in terms of the capability to separate multi-path components, and to overcome this limitation a new algorithm that operates iteratively was proposed that allows improvement of the time resolution. The algorithm performance was improved by including a threshold operation intended to estimate the number of effective multi-path components and minimize the probability of detecting false paths. Simulations performed using this algorithm on a UMTS-TDD chain have shown that the effect of Burst type on BER performance is negligible, and therefore for propagation scenarios with maximum delay lower than 6.2 *m*s we propose to use Burst-Type 2 in uplink transmission even $K=8$ users.

An extension for antenna arrays of the SMET estimation algorithm, based on a ML criterion was proposed, and its performance assessed. The proposed algorithm reduces the ML problem to KxL successive 3-dimensional maximization problem, computationally acceptable. The results have shown that the *DOA* accuracy estimation of the proposed ML algorithm improves when the threshold process is used on SMET. It was verified that the proposed ML-*DOA* estimation algorithm guarantees a *DOA* rms-error below 3º, for single user, even for multi-path components with temporal spacing between consecutive paths equal to one chip time interval, and any angular separation, and that for moderate to high values of Eb/n_0 the algorithm performance is close to the Crámer-Rao Bound.

This algorithm solves efficiently the complex problem of *DOA* estimation of multiple users in a multi path propagation environment even when the number of required *DOA's* exceeds the number of antenna array elements. Another property of the proposed algorithm is its ability to resolve signals from different users arriving from the same direction. This is due to processing in both time and space dimensions-if the signals from a number of users arrive from the same direction, they can still be separated in the time domain provided their midamble codes are different, and hence their respective *DOA's* can be estimated.

APPENDIX A

CRÁMER-RAO BOUND FORMULATION FOR AMPLITUDE AND DELAY ESTIMATION

The derivation of the *CRB* is based on computing the gradient of the log-likelihood function with respect to the unknown parameter vector, u [22] with Z elements. The estimation algorithm is based on the observation vector $\vec{r}$. Vector $\hat{u}$ is an unbiased estimator of deterministic unknown vector parameters u; hence E[$\hat{u}$] = u. According to the *CRB*, the mean square error satisfies:

$$E\left[\left(\hat{u}_i(\vec{r}) - u_i \right)^2 \right] \geq J^{ii} \qquad \text{(A1)}$$

where J^{ii} is the (i,i) element of the ZxZ square matrix J^{-1}. J is the ZxZ Fisher information matrix given by:

$$J = \left[J_{ij} \right] = \left[-E\left[\frac{\partial^2 \ln \Lambda(\vec{r} \mid u)}{\partial u_i d\, u_j} \right] \right] \qquad \text{(A2)}$$

where $\Lambda(\vec{r} \mid u)$ is the log-likelihood function of the observed vector $\vec{r}$ with respect to u.

A t wo-path channel with real amplitudes a_1, a_2 and delays t_1, t_2 is used as a basis for *CRB* calculation, thus u=[a_1 a_2 t_1 t_2]. The observation vector ($\vec{r}_w$), is the W_k chip window with Q=$L_M N_c/K$ samples, where L_M is the length of basic midamble code M, that is, 456 for Burst-Type 1 and 192 for Burst-Type 2. Therefore the log-likelihood function can be expressed as:

$$\ln \Lambda(W_k / u) = C - \frac{1}{2\sigma_n^2} \sum_{q=0}^{Q-1} \left[W_k(q) - a_1 G\left(q\frac{T_c}{N_c} - t_1 \right) - a_2 G\left(q\frac{T_c}{N_c} - t_2 \right) \right] \qquad \text{(A3)}$$

with

$$\sigma_n^2 = \frac{n_0}{2} \int_{-\infty}^{+\infty} \left| R(f) \right|^2 df \qquad \text{(A4)}$$

where C is some constant and $R(f)$ is the Fourier transform of the impulse response of the raised cosine filter: $R(f) = F\{G(t)\}$. After some mathematical manipulations the 4x4 Fisher information matrix be written as,

$$J = \begin{bmatrix} J_{11} & J_{12} & 0 & J_{14} \\ J_{12} & J_{11} & J_{23} & 0 \\ 0 & J_{23} & J_{33} & J_{34} \\ J_{14} & 0 & J_{34} & J_{44} \end{bmatrix} \quad \text{(A5)}$$

where,

$$J_{11} = \frac{1}{s_n^2} \int g^2(t) dt \quad \text{(A6)}$$

$$J_{12} = \frac{1}{s_n^2} \int g(t - t_1) g(t - t_2) dt \quad \text{(A7)}$$

$$J_{14} = \frac{a_2}{s_n^2} \int g(t - t_1) g'(t - t_2) dt \quad \text{(A8)}$$

$$J_{23} = \frac{a_1}{s_n^2} \int g'(t - t_1) g(t - t_2) dt \quad \text{(A9)}$$

$$J_{33} = \frac{a_1}{s_n^2} \int g'(t)^2 dt \quad \text{(A10)}$$

$$J_{34} = \frac{a_1 a_2}{s_n^2} \int g'(t - t_1) g'(t - t_2) dt \quad \text{(A11)}$$

$$J_{44} = \frac{a_2}{s_n^2} \int g'(t)^2 dt \quad \text{(A12)}$$

where $(.)'$ represents the derivative operation with respect to t.

Then the *CRB* of the parameters a_1, a_2, t_1, and t_2 are the elements of the diagonal of J^{-1} matrix,

$$J^{-1} = \begin{bmatrix} CRBa_1 & x & x & x \\ x & CRBa_2 & x & x \\ x & x & CRBt_1 & x \\ x & x & x & CRBt_2 \end{bmatrix} \quad \text{(A13)}$$

If $g(t)$ is the impulse response of the root raised cosine filter with factor 0.22, it is easy to demonstrate,

$$\lim_{t2-t1\to\infty} CRBa_1 = \lim_{t2-t1\to\infty} CRBa_2 = s_n^2$$
$$\lim_{t2-t1\to\infty} CRBt_1 \approx \frac{s_n^2}{2.8a_1^2};\ \lim_{t2-t1\to\infty} CRBt_2 \approx \frac{s_n^2}{2.8a_2^2} \quad \text{(A14)}$$

APPENDIX B

MAXIMUM LIKELIHOOD PARAMETERS ESTIMATION

The *M* sources error are assumed to be statistically independent. The application of ML criterion for estimation the unknown parameter vector $u=[a_l,\ f_l,\ q_l]$ seeks to find the maximum of the conditional probability function:

$$P(\vec{h}_l \mid u) = \prod_{m=0}^{M-1} \frac{1}{\sqrt{2p}\,s_\Delta} \exp\left[-\frac{1}{2s_\Delta^2} \left| \Psi_{l,m} - a_l\, e^{\,jq_l}\, e^{\,ja_m(f_l)} \right|^2 \right] \quad \text{(B1)}$$

that is,

$$P(\vec{h}_l \mid u) = \frac{1}{\left(2ps_\Delta^2\right)^{M/2}} \exp\left[-\frac{1}{2s_\Delta^2} \sum_{m=0}^{M-1} \left| \Psi_{l,m} - a_l\, e^{\,jq_l}\, e^{\,ja_m(f_l)} \right|^2 \right] \quad \text{(B2)}$$

The ML process of (B2) results in Minimum Mean Square Error (MMSE) criterion,

$$(\hat{a}_l, \hat{f}_l, \hat{q}_l) = \arg\min_{a_l, f_l, q_l} \sum_{m=0}^{M-1} \left| \Psi_{l,m} - a_l e^{jq_l} e^{ja_m(f_l)} \right|^2 \quad \text{(B3)}$$

where,

$$\sum_{m=0}^{M-1} \left| \Psi_{l,m} - a_l e^{jq_l} e^{ja_m(f_l)} \right|^2 = \sum_{m=0}^{M-1} \left(\Psi_{l,m} - a_l e^{jq_l} e^{ja_m(f_l)} \right)\left(\Psi_{l,m}^* - a_l e^{-jq_l} e^{-ja_m(f_l)} \right) \quad \text{(B4)}$$

$$\sum_{m=0}^{M-1} \left| \Psi_{l,m} - a_l e^{jq_l} e^{ja_m(f_l)} \right|^2 = \sum_{m=0}^{M-1} \left\{ \left| \Psi_{l,m} \right|^2 + a_l^{\,2} - \left(\Psi_{l,m} a_l e^{-jq_l} e^{-ja_m(f_l)} + \Psi_{l,m}^* a_l e^{jq_l} e^{ja_m(f_l)} \right) \right\} \quad \text{(B5)}$$

$$\sum_{m=0}^{M-1}\left|\Psi_{l,m}-a_l e^{jq_l}e^{ja_m(f_l)}\right|^2=\sum_{m=0}^{M-1}\left|\Psi_{l,m}\right|^2+Ma_l{}^2-2a_l\sum_{m=0}^{M-1}\text{Real}\left\{\Psi_{l,m}e^{-jq_l}e^{-ja_m(f_l)}\right\} \qquad \text{(B6)}$$

The first item of second term in (B6) does not depend of unknown parameter vector *u*, thus it can be seen that minimization operation in (B3) is equivalent to maximization the following Φ function,

$$\Phi(q_l,f_l,a_l)=2a_l\sum_{m=0}^{M-1}\text{Real}\left[\Psi_{l,m}e^{-jq_l}e^{-ja_m(f_l)}\right]-Ma_l{}^2 \qquad \text{(B7)}$$

$$\frac{\partial\Phi}{\partial q_l}=0\,;\frac{\partial\Phi}{\partial f_l}=0\,;\frac{\partial\Phi}{\partial a_l}=0\,; \qquad \text{(B8)}$$

and after solving (B8) we get:

$$\tilde{a}_l=\frac{1}{M}\sum_{m=0}^{M-1}\hat{a}_{l,m} \qquad \text{(B9)}$$

$$(\hat{f}_l,\hat{q}_l)=\arg\max_{f_l,q_l}\sum_{m=0}^{M-1}\hat{a}_{l,m}\cos\left(q_l+a_m(f_l)-\hat{\Omega}_{l,m}\right) \qquad \text{(B10)}$$

APPENDIX C

CRÁMER-RAO FORMULATION FOR *DOA* ESTIMATION

For the *DOA* estimation process the observation vector ($\vec{h}_l$), was defined by (14), thus the log-likelihood function with respect to the unknown parameter vector $u=[a_l, f_l, q_l]$ can be written as:

$$\ln\Lambda(\vec{h}_l\,|\,u)=C-\frac{1}{2s_\Delta^2}\sum_{m=0}^{M-1}\left|\Psi_{l,m}-a\,e^{jq_l}e^{ja_m(f_l)}\right|^2 \qquad \text{(C1)}$$

where *C* is some constant. For an array with *M* antenna elements the log-likelihood function is given by:

$$\ln \Lambda(\vec{h}_l \mid u) = C - \frac{1}{2s_{\Delta}^{2}}\left\{\sum_{m=0}^{M-1} \hat{a}_{l,m}{}^{2} + M a_l{}^{2} - 2a_l \sum_{m=0}^{M-1}(\hat{a}_{l,m}\cos(q_l + a_m(f_l) - \hat{\Omega}_{l,m})\right\} \quad \text{(C2)}$$

Thus,

$$J_{11} = -E\left[\frac{\partial^2 \ln \Lambda(\vec{h}_l)}{\partial q_l^2}\right] \quad J_{12} = -E\left[\frac{\partial^2 \ln \Lambda(\vec{h}_l)}{\partial q_l \partial f_l}\right] \quad \text{(C3)}$$

$$J_{13} = -E\left[\frac{\partial^2 \ln \Lambda(\vec{h}_l)}{\partial q_l \partial a_l}\right] \quad J_{21} = -E\left[\frac{\partial^2 \ln \Lambda(\vec{h}_l)}{\partial f_l \partial q_l}\right] \quad \text{(C4)}$$

$$J_{22} = -E\left[\frac{\partial^2 \ln \Lambda(\vec{h}_l)}{\partial f_l^2}\right] \quad J_{23} = -E\left[\frac{\partial^2 \ln \Lambda(\vec{h}_l)}{\partial f_l \partial a_l}\right] \quad \text{(C5)}$$

$$J_{31} = -E\left[\frac{\partial^2 \ln \Lambda(\vec{h}_l)}{\partial a_l \partial q_l}\right] \quad J_{32} = -E\left[\frac{\partial^2 \ln \Lambda(\vec{h}_l)}{\partial a_l \partial f_l}\right] \quad \text{(C6)}$$

$$J_{33} = -E\left[\frac{\partial^2 \ln \Lambda(\vec{h}_l)}{\partial a_l^2}\right] \quad \text{(C7)}$$

Then the *CRB* of the parameters q_l, f_l, and a_l are the elements of the diagonal of J^{-1} matrix,

$$J^{-1} = \begin{bmatrix} CRBq_l & x & x \\ x & CRBf_l & x \\ x & x & CRBa_l \end{bmatrix} \quad \text{(C8)}$$

REFERENCES

[1] M. Haardt, A. Klein, R. Koehn, S. Oestreich, M. Purat, V. Sommer and T. Ulrich, "The TD-CDMA Basead UTRA TDD mode", IEEE J. on Selected Areas in Comm., vol. 18, pp. 1375-1385, August 2000.

[2] S. Verdú, "Multiuser Detection", Cambridge University Press, 1998.

[3] A. Naguib, “Adaptive Antennas for CDMA Wireless Networks”, Ph.D. Thesis, Standford University, August 1996.

[4] E. Murray, “Performance of Network-Based Mobile Location Techniques within the 3GPP UTRA-TDD standards”, presented at the Proc. IEE 3G Mobile Comm. Technologies Conf., London, May 2002.

[5] 3GPP TS 25.221, “Physical channels and mapping of transport channels onto physical channels (TDD)”.

[6] J. C. Liberti, T. S. Rappaport, “Smart Antennas for Wireless Communications: IS-95 and Third Generation CDMA Applications”, Prentice Hall, 1999.

[7] 3GPP TS 25.201, “Physical Layer-General Description”.

[8] J. G. Proakis, “Digital Communications”, 3rd ed. New York: McGraw-Hill, 1995.

[9] InterDigital Communications Corporation,“ Complexity analysis of the multi-user channel estimation in TDD”, 3GPP TSG-RAN WG1 #5, 1999.

[10] ETSI, “Universal Mobile Telecommunications System, Selection procedures for the choice of radio transmission technologies of the UMTS”, TR 101112, pp. 42-43, 1998.

[11] P. Patel and J. Holtzmann, “Analysis of a simple successive interference cancellation scheme in DS/CDMA systems”, IEEE J. Selec. Areas Commun., June 1994.

[12] S. Lasaulce, P. Loubaton, E. Moulines, S. Buljore, “Training-based channel estimation and de-noising for the UMTS-TDD mode”, presented at IEEE VTC Fall, Oct. 2001.

[13] L.M. Correia (Editor), “*Wireless Flexible Personalised Communications*”, John Wiley & Sons, 2001.

[14] Lucent, Nokia, Siemens, Ericsson, “A standardized set of MIMO radio propagation channels”, 3GPP TSG-RAN WG1 #23, 2001.

[15] B. Tomiuk and N. Beaulieu, “General Forms for Maximal Ratio Diversity with Weighting Errors”, IEEE Trans. on Commun., Vol. 47, No 4, April 1999.

[16] R. Buehrer, N. Mendonza, B. Woerner, “A Simulation Comparison of Multiuser Receivers for Cellular CDMA”, IEEE Trans. on Vehicular Technology, Vol. 49, No. 4, July 2000, pp 1065-1085.

[17] A. Silva, P. Pinho, P. Marques, A. Gameiro, J. Fernandes, “Performance and Sensitivity Evaluation of Multisensor Parallel Interference Cancellation for the UMTS-TDD Uplink”, presented at the Proc. IST Mobile Comm. Summit, Barcelona, Spain, Sep. 2001.

[18] P. Marques, A. Gameiro, J. Fernandes, "Channel Estimation with Array Processing for the Uplink of UMTS-TDD", presented at the IEEE International Symposium on Personal, Indoor and Mobile Radio Communications, Lisboa, Sep. 2002.

[19] K. AlMidfa, "Performance evaluation of direction-of- arrival (*DOA*) estimation algorithms for mobile communication systems", presented at the IEEE Vehicular Tech. Conf, Tokyo 2000.

[20] C. Sengupta, J. Cavallaro and B. Aazhang, "On Multipath Channel Estimation for CDMA Systems Using Multiple Sensors", IEEE Trans. Comm., vol. 49, No 3, pp. 543-553, Mar 2001.

[21] E. Ertin, U. Mitra, S. Siwamogsatham, "Maximum-Likelihood-Based Multipath Channel Estimation for Code-Division Multiple-Access Systems", IEEE Trans. Comm., vol. 49, No 2, pp. 290-302, Feb 2001.

[22] J. Caffery, "*Wireless location in CDMA cellular radio systems*", Kluwer Academic Publishers, 2000.